International Journal of Physics and Mathematical Sciences ISSN: 2277-2111 (Online)
An Online International Journal Available at http://www.cibtech.org/jpms.htm
2013 Vol. 3 (4) October-December, pp.144-151/Rajkumar and Alagar

Research Article

TEXTURAL AND MORPHOLOGICAL ANALYSIS STUDIES OF ZINC ELECTRODEPOSITS FILMS

***S R Rajkumar[1] and M Alagar[2]**
[1]Department of Physics, Rajapalayam Rajus' College, Madurai Kamaraj University, Rajapalayam-626117, Tamil Nadu, India
[2]Department of Physics, Ayya Nadar Janaki Ammal College (Autonomous), Madurai Kamaraj University, Sivakasi -626124, Tamil Nadu, India
**Author for Correspondence*

ABSTRACT
Zinc and Zinc oxide (ZnO) thin films were electrodeposited at various bath temperatures (30-80° C). Structural characterization indicated the formation of polycrystalline Zn and ZnO film with hexagonal wurtzite structure of preferred c-axis orientation. The X- ray line profile analysis by the method of variance has been used to evaluate the micro structural parameters such as, crystallite size, RMS micro strain, dislocation density and stacking fault probability. The effect of film thickness and bath temperature on the micro structural parameters was analyzed. The FESEM examination reveals the nodular surface morphology and the results are well conversed.

Key Words: *Structural Characterization, Polycrystalline Zn, Surface Morphology, Dislocation Density, Stacking Fault Probability*

INTRODUCTION
Electrochemical deposition of metal and its oxide thin films has been an increasingly active research area in recent years. Zinc and its oxide are promising material for different applications such as solar cells, gas sensors, ultrasonic oscillators and transducers (Belghi *et al.,* 1991; Olvera *et al.,* 1993). More-over, ZnO is a good substitute in solar cells due to its high stability. While a number of techniques such as ion-assisted cyclic sputtering, r.f. sputtering, radio frequency plasma and chemical bath deposition have been applied to the fabrication of Zn films, in particular, the electrode-position method has advantages over other processes because of its simplicity and low equipment cost (Dalchiele *et al.,* 2001). Furthermore, the electrochemical process allows the coating over large areas with good lateral control of the material quality; even as such characteristic is readily achievable by electrodeposition, it is not yet possible or difficult with other state-of-the-art low temperature methods. This purpose of work is to contribute to this area by a summary of recent experimental studies on Zn thin films on tin- coated substrates. Most of the research workers have dealt with the determination of structure type and a qualitative observation of the defects and grain size of zinc oxide thin films. No quantitative measurements were attempted on the micro structural parameters of electrodeposited ZnO thin films. In the present work, the studies of several micro structural parameters of ZnO thin films, such as size of crystallites, micro strain, dislocation density and stacking fault probability using x-ray line profile are analyzed.

MATERIALS AND METHODS
Experimental Details
ZnO thin films were prepared from a 0.1 M zinc nitrate aqueous solution using deionized, de-mineralized water. The deposition was performed in a conventional three electrode cell using a Potentiostat -AutoLab PGSTAT 30 electrochemical analyzer (The Netherlands make). With glass plate as working electrode and a graphite rod as counted electrode. A saturated calomel electrode (SCE) with its Luggin capillary probe (Eliezer, 1993) located nearer to the cathode served as the reference electrode (Figure 1.1). All potentials were measured with reference to the potential of SCE. The cathodic potential at which the formation of thin film ZnO occurs was found to be –1.2 V (SCE), from cyclic voltammetry studies. The plating

experiments were carried out from 30 to 90 ° C with every 30 seconds at a given cathodic current density different intervals of time. Uniform, smooth ZnO films were obtained under optimized conditions and the films were well adherent to the substrates.

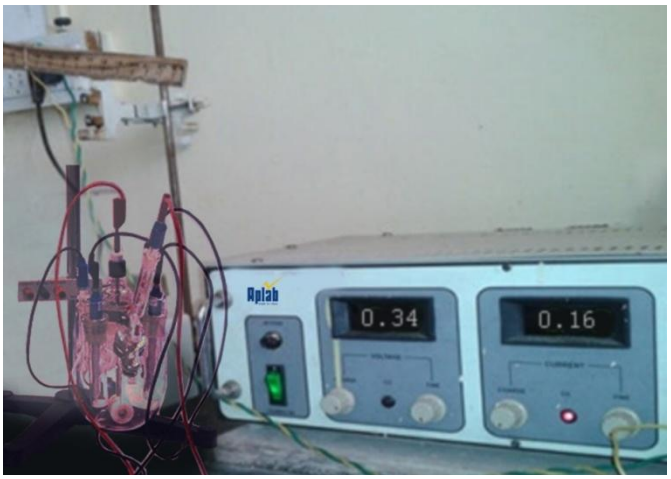

Figure 1.1: Photograph of Schematic of full experimental system with saturated calomel electrode (SCE) Setup

The thickness of the films was estimated using a multiple beam interferometer and weight loss method in the appropriate ranges. X-ray diffraction data of the electrodeposited samples were recorded using XRD, PANalytical X'Pert PRO diffractometer with Cu Kα radiation (λ =1.54A^0) at the X-ray scan rate was 1min^{-1} for 2θ ranging from 10^0 to 90^0 and A field emission scanning electron microscope (FESEM) (JEOL- JSM 6701F) was used to examine the grain size (>1μm) of the coated surface and cross-sectional morphologies of the nanocrystalline zinc deposits. Calculation of crystallite size and micro strain were made using variance analysis of X-ray line profiles. Dislocation densities are calculated from the particle size and R.M.S strain values, using the relations given by Williamson and Smallman (1956). The stacking fault probabilities were calculated from the peak shift, using the relations given by Warren and Warekois (1955).

RESULTS AND DISCUSSION

Structural analysis

Figure 1 shows the x-ray diffraction pattern obtained for 1 μ m thick ZnO film deposited at –1.1 V (SCE) and bath temperature 80° C. All the peaks identified are from ZnO and no additional lines corresponding to Zn and other oxides are present. It was also evident from these diffractogram that the (002) reflections are of maximum intensity, indicating thereby a strong orientation with stacking of the planes along the c-axis. This indicates that electro-deposition method is useful for the preparation of single phase ZnO. The planes have been observed and compared with the JCPDS files (Eugene *et al.*, 2003; Bauer *et al.*, 2011; Zhang and Koch, 2000; Berube and Esperence, 1989). The calculated 'd' values are found to be in good agreement with the JCPDS file for hexagonal ZnO (JCPDS, 1992). This clearly indicates that the material of the prepared films is pure Zn with hexagonal wurtzite type structure. The effect of preparation conditions (like deposition potential) on the orientation of the polycrystalline films are investigated by evaluating the texture coefficient T_c (hkl) using the following relation (Hadouda *et al.*, 1995).

$$T_c = \frac{I(hkl)/I_o(hkl)}{\left(\frac{1}{N}\right)[\Sigma_N I(hkl)/I_o(hkl)]}$$

Research Article

Where $T_{c(hkl)} -$ is the texture coefficient of the (hkl) plane, $I -$ is the measured intensity, $I_o -$ is the JCPDS standard intensity and $N -$ is the number of diffraction peaks. From the above equation, it is seen that, the texture coefficient approaches unity for a randomly distributed sample, while $T_c -$ is larger than unity when the (hkl) plane is preferentially oriented. The variation of texture coefficient of Zn films deposited at various cathodic potentials with bath temperature 80° C is shown in Figure 2. It is seen that, the preferred orientation of Zn films changes from (101) to (002) plane with the increase of cathodic potential (–0.8 to –1.2 V versus SCE). The increase in preferred orientation is attributed with the increased number of grains along the plane. The lower values of texture coefficient reveals that the films have poor crystallinity and the crystallinity may be improved by higher temperatures annealing.

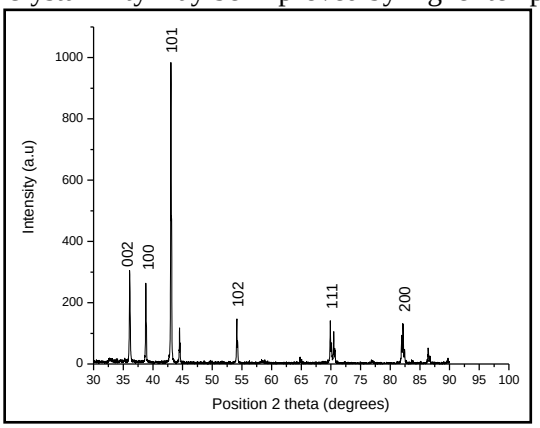

Figure 1: X-ray diffraction pattern of electrodeposited Zn thin film at bath temperature 80°C

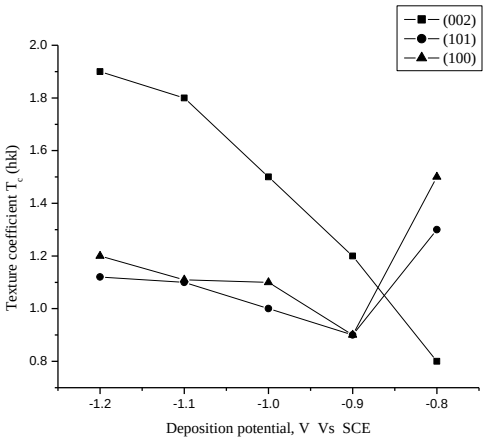

Figure 2: Variation of texture coefficient along the planes (100), (101) and (002) of ZnO films at deposition temperature 80°C

Crystalline profiles and variance analysis

For the calculation of crystallite size and micro strain, the line profiles are subjected to variance analysis (Mitra, 1965). Since the variances are additive, the profiles were corrected for instrumental broadening by subtracting the variance of the corresponding profile for standard well annealed Zn samples. If it is assumed that the broadening of the x-ray line is due to the crystallite size and strain only, the variance can be written as

$$W_{2\theta} = \left[\frac{\lambda\sigma}{2\pi^2 P cos\,\theta_B}\right] + 4\,tan^2\theta < e^2 > [1]$$

Where $\lambda -$ is the wavelength of x-rays, $\sigma -$ the angular range (in 2θ) over which the intensity distribution is appreciable, $P -$ the crystallite size, $\theta -$ the Bragg angle and $< e^2 >$- is the mean square strain.

However, variance is a range sensitive parameter and consequently depends on the choice of the background level which has a marked influence on the range to be selected for integration. In fact, it is found that the diffraction profiles approach zero, rather asymptotically following an inverse square law. For such a function varying inversely as the square of the distance from the mean, the variance will be a linear function of the total range σ and can be written as, $W = K\sigma + C$, where K and C are constants and are dependent on the physical conditions of the sample and the geometrical factors. Dislocation density is defined as (Hirsch, 1956) the length of dislocation line per unit volume of the crystal. The dislocation density is calculated using the following relation (Williamson and Smallman, 1956),

$$\rho = \frac{(\frac{3nK}{F})^{1/2} < e^2 >^{1/2}}{bp} [2]$$

where n, the number of dislocations on each face of the particle, K the constant depending on the strain distribution, F is an interaction parameter, $< e^2 >^{1/2}$ the RMS strain, b the Burgers vector and p the crystallite size. For Cauchy strain profiles the value of K is about 25, whereas for Gaussian strain profiles it is nearly 4. In the absence of extensive polygonization, dislocation density can be calculated from the above Equation (2), by assuming n ≈F, b = d, the interplanar spacing and K = 4. Now the Equation (2) reduces to

$$\rho = \sqrt{12}\ < e^2 >^{1/2} / dp [3]$$

The stacking fault probability α is the fraction of layers undergoing stacking sequence faults in a given crystal and hence one fault is expected to be found in 1/ α layers. The presence of stacking faults gives rise to a shift in the peak positions of different reflections with respect to ideal positions of a fault-free well annealed sample. Four typical experimental profiles showing the peak shift for hexagonal (002) reflection of Zn films at different bath temperatures with respect to a well annealed sample are shown in Figure 3. A well annealed sample reference is used to compare the shift in the peak position of different reflections and hence to evaluate the micro structural parameters. The relation connecting stacking fault probability (α) with peak shift Δ (2θ) was given by Warren and Warekois (1955).

$$\alpha = \left[\frac{2\pi^2}{45}\sqrt{3}\right] [\Delta(2\theta) / \tan\theta_{002}] [4]$$

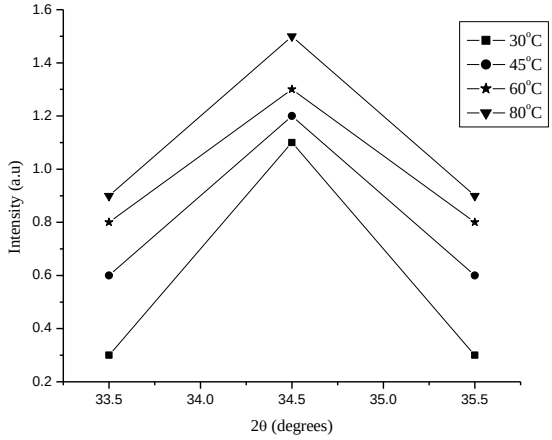

Figure 3

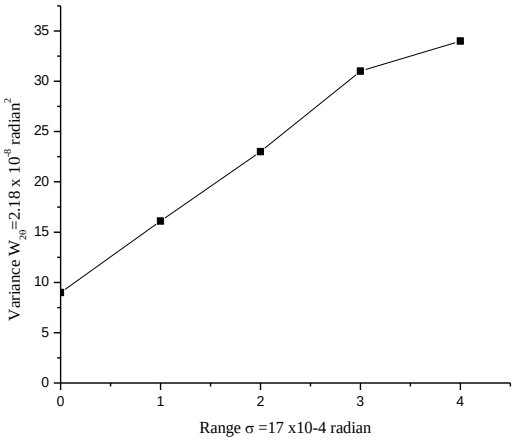

Figure 4

Figure 3: X-ray diffraction profiles showing the peak shift and line broadening. a) 30°C, b) 45°C, c) 60°C d) 80°C. The vertical line indicates the position of the annealed sample

Figure 4: Relation connecting the variance and angular range for Zn film of thickness 1µm deposited at bath temperature 80°C

From the above expression (4) the stacking fault probability was calculated by measuring the peak shift with the well annealed sample. Figure 4 shows the typical variance plot $W_{2\theta}$ as ordinate against range (σ) as abscissa for a typical film of 1μm thickness deposited at bath temperature 80°C. The emphasis was given here to the points corresponding to the tail because of their great sensitivity towards variance. The linearity of the graph confirmed that the background has been adjusted properly and it also established the correctness of the data.

Micro structural parameters of Zn films

The micro structural parameters of Zn films deposited at different bath temperatures with constant deposition time (30 minutes) are given in table 1 and table 2.

Table 1: Micro structural parameter of Zn deposits for different bath temperatures and film thickness. Deposition time: 30 minutes, Solution pH : 3.5 ± 0.1

Bath temperature(°C)	Film thickness t(μm)	Crystallite size p(μm)	RMS Microstrain $<e^2>^{1/2}\times10^{-4}$	Dislocation density $\times10^{14}$(lines/m^2)	Stackingfault probability α
30	600	54.5	41.47	9.24	0.060
45	710	56.5	33.75	8.37	0.043
60	1100	64.1	32.44	6.22	0.071
80	1230	73.2	31.25	5.26	0.074

Table 2: Microstructural variations of Zn films for different deposition times and film thickness. Deposition temperature: 8 0°C, Solution pH : 3.5 ± 0.1

Deposition time(mins)	Film thickness t(μm)	Crystallite size p(μm)	RMS Microstrain $<e^2>^{1/2}\times10^{-4}$	Dislocation density $\times10^{14}$(lines/m^2)	Stackingfault probability α
5	220	54.5	42.22	11.37	0.090
10	330	56.5	41.47	16.22	0.083
20	760	64.1	33.75	9.24	0.071
30	910	73.2	32.44	8.37	0.074
45	1100	64.1	31.25	6.22	0.060
60	1230	73.2	31.25	5.26	0.043

Plots showing the variation of particle size, R.M.S strain, dislocation density and stacking fault probability with bath temperature are presented in Figure 5 and Figure 6. Figure 5 represents the variation of crystallite size and micro strain with bath temperature. It is observed from the Figure 5 that the crystallite size increases gradually with bath temperature and attained a maximum value of 72.4 nm at a bath temperature of 80° C. On the other hand, the R.M.S. micro strain decreases with increase of bath temperature and reached a minimum value of $31x10^{-4}$ for a typical Zn film deposited at 80°C. Due to the increase in crystallite size with bath temperature, the defects in the lattice are reduced, which in turn, reduces the R.M.S micro strain. From the Figure 6, it has been observed that, both dislocation density and the stacking fault probability decreases with increasing bath temperature. Moreover, due to the increase of bath temperature, stresses in the layers and hence the number of dislocation lines cutting unit area decreases from 9.74 to 5.72. Due to the release of stresses built-up in the layers, the variation of interplanar spacing decreases which finally lead to a decrease in stacking fault probability from 0.08 to 0.024 for films deposited at a bath temperature of 80° C. The analysis on the effect of bath temperature indicate that the crystallite size increases with bath temperature whereas R.M.S. micro strain, dislocation density and stacking fault probability decreases. The variation of crystallite size and micro strain with film thickness is shown in the Figure 7.

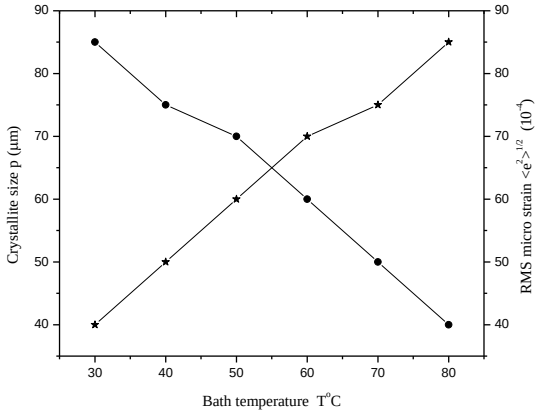

Figure 5

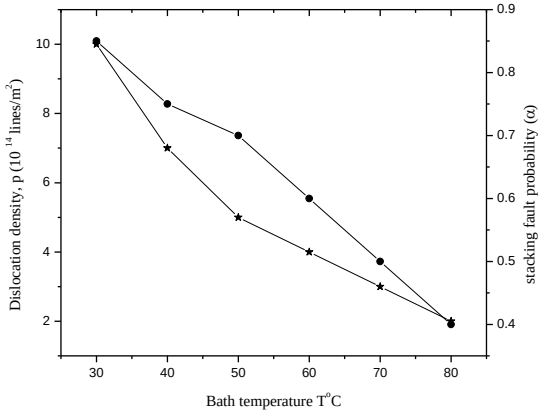

Figure 6

Figure 5: Variation of crystallite size and R.M.S microstrain with bath temperature for Zn films Figure 6: Variation of dislocation density and stacking fault probability with bath temperature for ZnO films

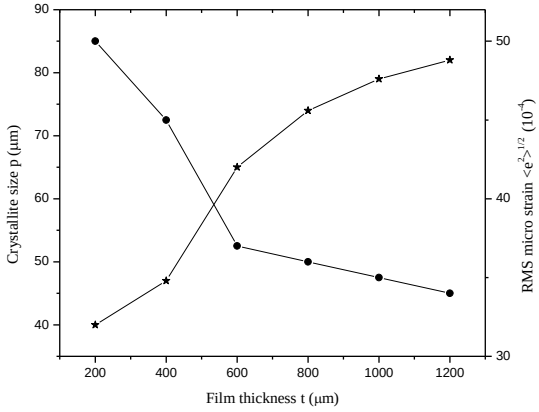

Figure 7

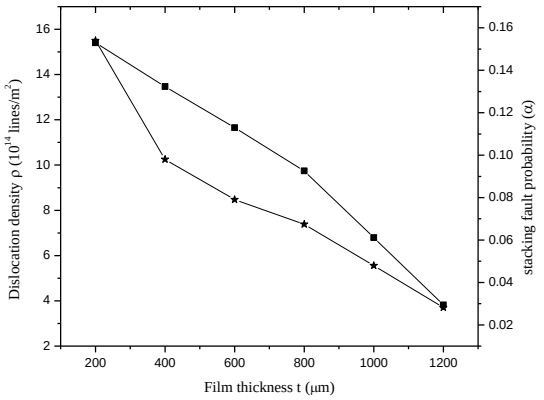

Figure 8

Figure 7: Variation of crystallite size and R.M.S microstrain with film thickness for Zn films
Figure 8: Variation of dislocation density and stacking fault probability with film thickness for ZnO films

Figure 8 represents the variation of dislocation density and stacking fault probability with film thickness for typical Zn films. It is observed from the above figures that the R.M.S micro strain, dislocation density and stacking fault probability are decreasing with increase in film thickness and minimum values are obtained for a film of thickness 1.1μm. The crystallite size is observed to increase with film thickness and a value of 75 nm is obtained for a film of thickness 1.1 μm. For thinner films, the micro strain, dislocation density and the stacking fault were found to be larger. More-over, during the building up of film thickness, the micro strain and dislocation density are reduced due to the release of stresses in the films. The cumulative effect of decrease in R.M.S strain and dislocation density may be responsible for the gradual reduction in stacking fault of the layers with increase in film thickness.

Surface morphology

A Field emission scanning electron micrograph (FESEM) of a representative 1.2 μm thick Zn film is shown in the Figure 9. The FESEM picture clearly illustrates the nodular structure of the film. The coating layer is dense with very fine crystals. The discontinuities appeared in the coating layer indicates that a significant amount of hydrogen gas evolved simultaneously at the cathode interfered with the crystal structure.

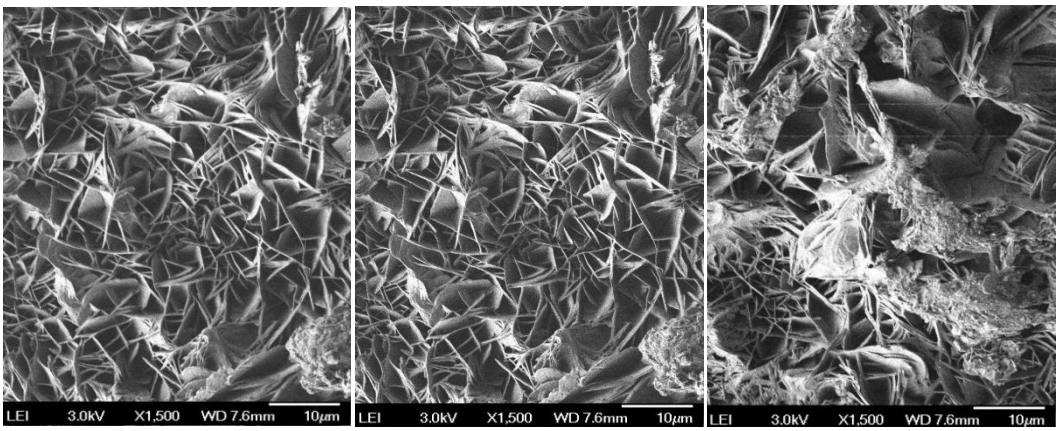

Figure 9: Typical FESEM picture of a Zn thin film deposited at 80^{o}C

Conclusion

Electrodeposited Zn films were obtained on conducting glass plates by cathodic electrodeposition process. The XRD analysis reveals the hexagonal wurtzite structure and the variation of texture coefficient for different cathodic potentials were studied. X-ray line broadening studies are carried out for films prepared at various bath temperatures. The micro structural parameters for the Zn and ZnO thin films were evaluated and they are found to depend on the film thickness and bath temperature. The R.M.S micro strain, dislocation density and stacking fault probability were found to decrease with film thickness, whereas, the crystallite size increases with film thickness. It is observed that the micro structural parameters exhibit a monotonic variation with bath temperature (30 – 80°C) and film thickness (0.21 - 1.2 μm) in the measurement ranges. The surface morphology of ZnO film illustrates that the surface was composed of the aggregates of a hexagonal columnar grains which had grown normal to the substrate surface.

REFERENCES

Bauer G, Gravemeier V and Wall WA (2011). A 3D finite element approach for the coupled numerical Simulation of electrochemical systems and fluid flow. *International Journal for Numerical Methods in Engineering* **86**(11) 1339–1359.

Belghi K, Subhan MA, Rulhe U, Duchemin S and Boughot J (1991). *Proceeding of 10th EC Photovoltaic Solar Energy Conference. Lissbon, Portugal. Available:* http://link.springer.com/book/10.1007/978-94-011-3622-8 ISBN: 978-94-010-5607-6 (Print) 978-94-011-3622-8 (Online) 613-621.

Berube Ph L and Esperance GL (1989). A Quantitative Method of Determining the Degree of Texture of Zinc Electrodeposits. *Journal of the Electrochemical Society* **136**(8) 2314-2315.

Dalchiele EA, Giorgi P, Marotti RE, Martin F, Ramos – Barrado JR, Ayouci R and Leinen D (2001). Electrodeposition of ZnO thin films on n-Si (1 0 0). *Solar Energy Materials and Solar Cells. C* **70**(3) 245-254.

Eliezer Giledi (1993). *Electrode kinetics* (VCH Publishers Inc, New York), **8** 45-50.

Eugene Malyshev, Uziel Landau, and Sergey Chivilikhin (2003). Modeling the Deposit Thickness Distribution in Copper Electroplating of Semicondutor Wafer Interconnects. Session TK. *Proceedings of the AICHE Annual Meeting, San-Francisco, CA.* Available: http://www.l-chem.com/publications.html. 190 c.

Hadouda H, Pouzet J, Bernede JC and Barreau A (1995). MoS_2 thin film synthesis by soft sulfurization of a molybdenum layer. *Materials Chemistry and Physics* **42**(4) 291-297.

Hirsch PB (1956). Mosaic Structure. *Progress in Metal Physics* **6** *236-339.*

International Center for Diffraction Data, Joint Committee on Powder Diffraction Standards (**JCPDS- 5-0664**, ZnO*)* (**1992**)

Mitra GB (1965). Determination of particle size and strain in a distorted polycrystalline aggregate by the method of variance. *Acta Crystallographica* **17** 765-766
Olvera de la ML, Maldonado A, Asomoza R, Konagai M and Asomoza M (1993). Growth of textured ZnO:In thin films by chemical spray deposition. *Thin Solid Films* **229**(2) *196*-200 .
Warren BE and Ware kois EP (1955). Stacking faults in cold worked alpha-brass. *Acta Metallurgica* **3**(5) 473-479.
Williamson GK and Smallman RE (1956). Dislocation densities in some annealed and cold worked metals from measurements on the X ray Debye Scherrer spectrum. *Philosophical Magazine* **1** 34-45.
Zhang X and Koch CC (2000). *129th Proceedings of International Symposium: The Metal and Materials Society (TMS), Nashville, Tennessee.* Available: http://www.tms.org/ pubs/books/ proceedings.aspx 289 - 298.